Residues in Na^+ Channel D3-S6 Segment Modulate both Batrachotoxin and Local Anesthetic Affinities

Sho-Ya Wang,* Carla Nau,† and Ging Kuo Wang†

*Department of Biology, State University of New York, Albany, New York 12222, and †Department of Anesthesia, Harvard Medical School and Brigham and Women's Hospital, Boston, Massachusetts 02115 USA

ABSTRACT Batrachotoxin (BTX) alters the gating of voltage-gated Na^+ channels and causes these channels to open persistently, whereas local anesthetics (LAs) block Na^+ conductance. The BTX and LA receptors have been mapped to several common residues in D1-S6 and D4-S6 segments of the Na^+ channel α-subunit. We substituted individual residues with lysine in homologous segment D3-S6 of the rat muscle μ1 Na^+ channel from F1274 to N1281 to determine whether additional residues are involved in BTX and LA binding. Two mutant channels, μ1-S1276K and μ1-L1280K, when expressed in mammalian cells, become completely resistant to 5 μM BTX during repetitive pulses. The activation and/or fast inactivation gating of these mutants is substantially different from that of wild type. These mutants also display ~10–20-fold reduction in bupivacaine affinity toward their inactivated state but show only approximately twofold affinity changes toward their resting state. These results demonstrate that residues μ1-S1276 and μ1-L1280 in D3-S6 are critical for both BTX and LA binding interactions. We propose that LAs interact readily with these residues from D3-S6 along with those from D1-S6 and D4-S6 in close proximity when the Na^+ channel is in its inactivated state. Implications of this state-dependent binding model for the S6 alignment are discussed.

INTRODUCTION

Voltage-gated Na^+ channels are responsible for generating action potentials in excitable membranes (Hille, 1992). Upon depolarization, the Na^+ channel enters an ion-conducting open state that is fast inactivated, generally within a millisecond. The fast-inactivated channel recovers rapidly within 10–30 ms upon repolarization. Prolonged depolarization from several seconds to a few minutes elicits additional slow inactivation of the Na^+ channel (Chandler and Meves, 1970), which recovers with a rather slow time course over a period of several minutes upon repolarization.

Mammalian voltage-gated Na^+ channels consist of one large α-subunit and one or two smaller auxiliary β-subunits (Catterall, 1995; Fozzard and Hanck, 1996). The Na^+ channel α-subunit cDNA clone, when expressed in a mammalian expression system, can form functional Na^+ channels with relatively normal activation and inactivation gating kinetics (Ukomadu et al., 1992). The α-subunit channel protein contains four homologous domains (D1–D4), each with six putative α-helical transmembrane segments (S1–S6) (Fig. 1 *A*). The fast inactivation gating of the Na^+ channel has been resolved in some detail. For example, the triplet IFM locus (isoleucine, phenylalanine, and methionine) in the intracellular linker region between D3 and D4 is thought to be a part of the "inactivation ball" (West et al., 1992). Two S4–S5 intracellular regions within D3 and D4, respectively, may together form the receptor for the IFM locus (McPhee et al., 1998; Smith and Goldin, 1997). The voltage sensor has been delimited at the S4 region, where multiple positively charged residues are present (e.g., Yang et al., 1996). In contrast, the activation gate and the slow inactivation process of the Na^+ channel are less clear at the molecular level, although some specific regions have been implicated in the modulation of these processes (e.g., Balser et al., 1996; Bennett, 1999; Vilin et al., 1999).

Batrachotoxin (BTX), an alkaloid neurotoxin (Fig. 1 *B*) that is most abundant in the skin of the South American frog *Phyllobates terribilis* (Daly et al., 1980), has been a useful molecular probe for Na^+ channel gating processes (Catterall, 1980; Strichartz et al., 1987; Brown, 1988). First, BTX modifies the Na^+ channel activation gating drastically; this Na^+ channel activator shifts the voltage dependence of activation to a hyperpolarizing direction by 30–50 mV. Second, both fast and slow inactivation processes of Na^+ channels are also inhibited by BTX. As a result, Na^+ channels open persistently in the presence of BTX, even at resting membrane potentials. The whereabouts of the BTX receptor were first determined by Trainer et al. (1996), who found, by a photoaffinity-labeling technique, that the D1-S6 segment was covalently linked to BTX. The receptor site for BTX was later delimited to three residues at the middle of segment D1-S6 (Wang and Wang, 1998). Recent studies demonstrated that three additional residues at the middle of segment D4-S6 are critical in BTX binding (Linford et al., 1998; Wang and Wang, 1999). How BTX alters the Na^+ channel gating via binding interactions remains unclear.

In contrast to the Na^+ channel activator BTX, local anesthetics (LAs) are clinical drugs that block Na^+ channels (Hille, 1992). The structure of a typical LA, bupivacaine, is shown in Fig. 1 *B*. LAs inhibit Na^+ currents tonically when the membrane is depolarized infrequently. In addition, LAs

Received for publication 9 March 2000 and in final form 19 May 2000.

Address reprint requests to Dr. Ging Kuo Wang, Department of Anesthesia, Brigham and Women's Hospital, 75 Francis St., Boston, MA 02115. Tel.: 617-732-6886; Fax: 617-730-2801; E-mail: wang@zeus.bwh.harvard.edu.

0006-3495/00/09/1379/09 $2.00

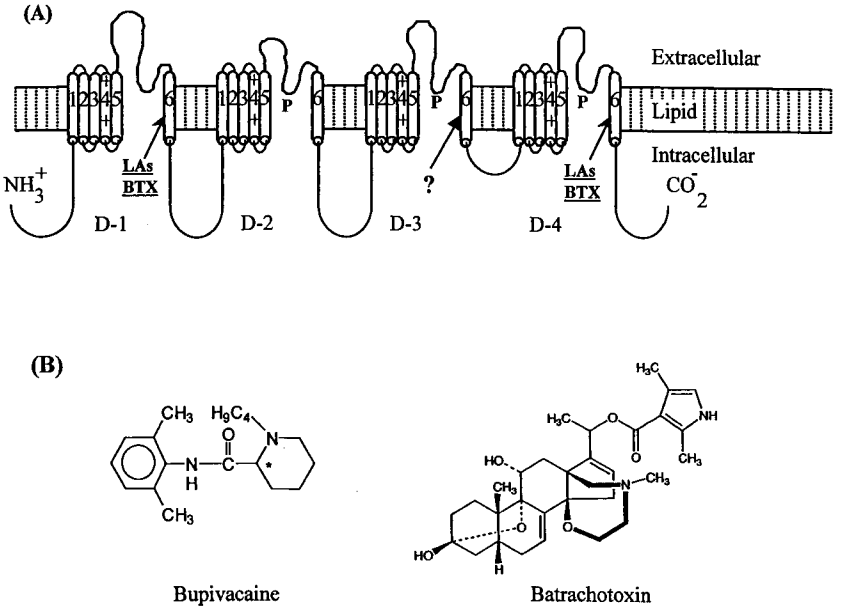

FIGURE 1 (*A*) The transmembrane organization of the Na^+ channel α-subunit. The arrows indicate the putative BTX binding site and the putative LA binding site at segments D1-S6 and D4-S6. The role of D3-S6 in BTX and LA binding is unknown, as labeled by a question mark. P designates the pore region within the S5-S6 extracellular linker. (*B*) Chemical structures of batrachotoxin (538 Da) and bupivacaine (288 Da). The chiral carbon in bupivacaine is marked by an asterisk. The S(−)-bupivacaine isomer has been used in clinical trials (Burke et al., 1999).

elicit additional use-dependent block of Na^+ currents during repetitive pulses. The detailed mechanism of this use-dependent phenomenon is uncertain, although the involvement of channel activation has been suggested (e.g., Wang et al., 1987; Hanck et al., 1994; Vedantham and Cannon, 1999). The first mapping of the LA receptor revealed that four residues at the middle of segment D4-S6 are critical for LA binding (Ragsdale et al., 1994). In fact, three common residues in D4-S6 are critical for binding of both BTX and LAs (Linford et al., 1998; Wang and Wang, 1999) (Fig. 2). Further studies suggested that two additional residues in the middle of segment D1-S6 are aligned in close proximity with the tertiary amine moiety of LAs (Wang et al., 1998; Nau et al., 1999), particularly when the channels are in their inactivated state. Again, these same residues are critical for binding to both BTX and LAs (Fig. 2). In addition to residues at D4-S6 and D1-S6, the P-region (located at the S5-S6 linker; Fig. 1 *A*), which controls the ion selectivity of Na^+ channels, may also be involved in LA binding (Sunami et al., 1997).

The binding of LAs and BTX with the Na^+ channel is highly state dependent. LAs bind preferentially to the inactivated state of Na^+ channels, whereas BTX binds to its receptor site when the channel is first in its open state (Hille, 1992). LAs also antagonize [^{3}H]BTX binding (Creveling et al., 1983). However, this antagonistic reaction between BTX and LA binding to Na^+ channels was suggested to be due to an indirect allosteric interaction of these two ligands (Postma and Catterall, 1984). This suggestion has been revised recently; the BTX receptor apparently shares overlapping molecular determinants with the LA receptor (Linford et al., 1998; Wang and Wang, 1999). In this study, we postulated that an additional S6 segment might participate in the binding of BTX and LAs. Because Na^+ channels contain four homologous domains, we tested this possibility by examining the role of segment D3-S6 in BTX and LA binding during state transitions.

MATERIALS AND METHODS

Site-directed mutagenesis

Point mutations of a μ1 Na^+ channel clone in a pcDNA1/Amp expression vector were performed as described (Nau et al., 1999), with a Transformer Site-Directed Mutagenesis Kit (Clontech). A mutagenesis primer and a restriction primer were used to generate the desired mutant. The potential

μ1 Na^+ channel	Position	1 5 10 15 20 25
D1	------S6 segment	YMIFF VVIIF LGSFY L**I**N**L**I L**A**VVA MAY--
D2	------S6 segment	CLTVF LMVMV IGNLV VL**N**LF L**A**LLL SSF--
D3	------S6 segment	MYLYF VIFII FG**S**FF T**L**NLF IGVII DNF--
D4	------S6 segment	GICFF CSY**I**I IS**F**LI VV**N**M**Y** IAIIL ENF--
		1 5 10 15 20 25

FIGURE 2 Amino acid sequences of S6 transmembrane segments in domains D1–D4. Residues critical for BTX binding are in bold letters (Wang and Wang, 1998, 1999; Linford et al., 1998). Residues critical for LA binding are underlined (Ragsdale et al., 1994; Wang et al., 1998). Notice that a total of five common residues within D1S6 and D4S6 are critical for both BTX and LA binding. The LA sensitivity of μ1-I433K was not studied.

mutants were selected and confirmed by DNA sequencing at the mutated site, using appropriate primers.

Transient transfection

The culture of Hek293t cells and their transient transfection were performed as described (Cannon and Strittmatter, 1993). Cells were first grown to 50% confluence in Dulbecco's minimum essential medium (GIBCO) containing 10% fetal bovine serum (HyClone), 1% penicillin and streptomycin solution (Sigma), 3 mM taurine, and 25 mM HEPES (GIBCO). Transfection of these cells with μ1 (10 μg) and reporter plasmid CD8-pih3m (1 μg) was accomplished by a calcium phosphate precipitation method in a Ti25 flask. Cells were replated 15 h after transfection, maintained at 37°C in a 5% CO_2 incubator, and used for experiments after 1–4 days. Transfection-positive cells were identified by immunobeads (CD8-Dynabeads, Lake Success, NY).

Whole-cell voltage clamp

The whole-cell configuration of a patch-clamp technique (Hamill et al., 1981) was used to record Na^+ currents in cells coated with CD8 immunobeads. Experiments were performed at room temperature (23 ± 2°C). Glass electrodes contained 100 mM NaF, 30 mM NaCl, 10 mM EGTA, and 10 mM HEPES adjusted to pH 7.2 with CsOH. The electrodes had a tip resistance of 0.5–1.0 MΩ; access resistance was generally <2–3 MΩ. With series resistance compensation of 60–90%, the voltage error at +50 mV was <4 mV on average. Series resistance errors of this magnitude are generally tolerable because quantitative measurements of current kinetics and drug block are insignificantly affected by such errors (Bean, 1992). The bath solution contained 65 mM NaCl, 85 mM choline chloride, 2 mM $CaCl_2$, and 10 mM HEPES adjusted to pH 7.4 with tetramethyl hydroxide. These ionic conditions resulted in smaller Na^+ currents at voltages from −60 to +10 mV, which in turn minimalized the series resistance artifact in the conductance-voltage measurement. A stock solution of bupivacaine was prepared at 100 mM in aqueous solution and stored at −20°C until needed. BTX was prepared at 0.5 mM in dimethyl sulfoxide and stored at 4°C. Bupivacaine enantiomers were kindly provided by Dr. Rune Sandberg (Astra Pain Control, Sodertalje, Sweden), and BTX was a generous gift of Dr. John Daly (National Institutes of Health, Bethesda, MD). To conserve the use of BTX, we included this toxin in the pipette solution at 5 μM final concentration when needed. This toxin concentration was previously used to demonstrate the BTX-resistant phenotype in poison-dart frogs (Daly et al., 1980) and was high enough to modify >90% of available Na^+ channels under appropriate conditions. Whole-cell currents were recorded with Axopatch 200B, filtered at 5 kHz, and collected by pClamp software (Axon Instruments, Foster City, CA). After gigaohm seal formation and establishment of whole-cell voltage clamp, the cells were dialyzed for ~20 min before data were acquired. Most of the capacitance and leakage current was canceled by the Axopatch 200B circuitry and further subtracted by the P/-4 method. An unpaired Student's *t*-test was used to evaluate estimated parameters (mean ± SEM or fitted values ± SE of the fit); p values of <0.05 were considered statistically significant.

RESULTS AND DISCUSSION

Mutations of μ1-S1276K and μ1-L1280K in D3S6 render Na^+ channels resistant to BTX

Individual residues from μ1-F1274 to μ1-N1281 within the putative α-helical segment D3-S6 were substituted with a lysine amino acid. This specific region was chosen because it is equivalent to the D4-S6 region where BTX-resistant mutants were found (Fig. 2). Introduction of a positively charged residue will in theory disrupt binding between this amino acid and the highly hydrophobic ligand BTX, provided that this residue is in close proximity during ligand binding. Only two of eight mutant channels with the lysine substitution expressed sufficient Na^+ currents for further experiments; these were μ1-S1276K and μ1-L1280K. The remaining mutants (F1274K, G1275K, F1277K, F1278K, T1279K, and N1281K) expressed little (<0.5 nA) or no Na^+ current. Cotransfection of β1 subunit clone with these mutant clones did not improve their expression level, except for one, μ1-F1274K (usually ~0.5 nA at +50 mV). It appeared that this region is rather sensitive to lysine substitution, in contrast to the homologous D1-S6 region, where 9 of 12 lysine mutants express sufficient Na^+ currents (Wang and Wang, 1998).

With 5 μM BTX included in the pipette solution, repetitive pulses readily promoted BTX binding to the open state of wild-type μ1 Na^+ channels (Fig. 3 *A*). A large portion of Na^+ currents, up to 80% of the corresponding peak current amplitude, was maintained at +50 mV after 1000 repetitive pulses. A corresponding large inward "tail" current was evident upon repolarization as the BTX-modified Na^+ channels quickly returned to their resting state. Under identical conditions, however, BTX at 5 μM failed to modify the currents of μ1-S1276K and μ1-L1280K mutant channels after 1000 pulses (representative traces in Fig. 3, *C* and *D*; $n = 7$). Additional pulses of up to 3000 total to these mutant channels did not add any noninactivating maintained currents. Clearly, both μ1-S1276K and μ1-L1280K Na^+ channels are completely BTX resistant. In contrast, the mutant μ1-F1274K Na^+ channels (cotransfected with β1 subunit) remain BTX sensitive in a manner comparable to that of wild-type μ1 channels (Fig. 3 *B*; $n = 5$). As control experiments, we found that cotransfection of β1 subunit with μ1-L1280K does not alter the BTX-resistant phenotype ($n = 5$ with pulses up to 3000 under identical conditions). This result suggests that β1 does not have a significant role in the BTX-resistant phenotype. Because the right-handed α-helical structure consists of 3.6 residues per turn, residues at μ1-S1276 and μ1-L1280, therefore, will be roughly at the same face of the α-helical structure, whereas residues at μ1-F1274 will be oriented in the opposite direction. Together with the findings from D1-S6 and D4-S6 mutants (Wang and Wang, 1998, 1999; Linford et al., 1998), our results from D3-S6 mutants strongly support the notion that homologous S6 segments indeed align in close proximity. In other words, residues at μ1-S1276 and μ1-L1280, like several residues in D1-S6 and D4-S6, are probably involved directly in binding to BTX.

Altered activation and/or inactivation gating in BTX-resistant mutant channels

To assess whether the mutant channels are altered in their gating properties, we characterized their activation and in-

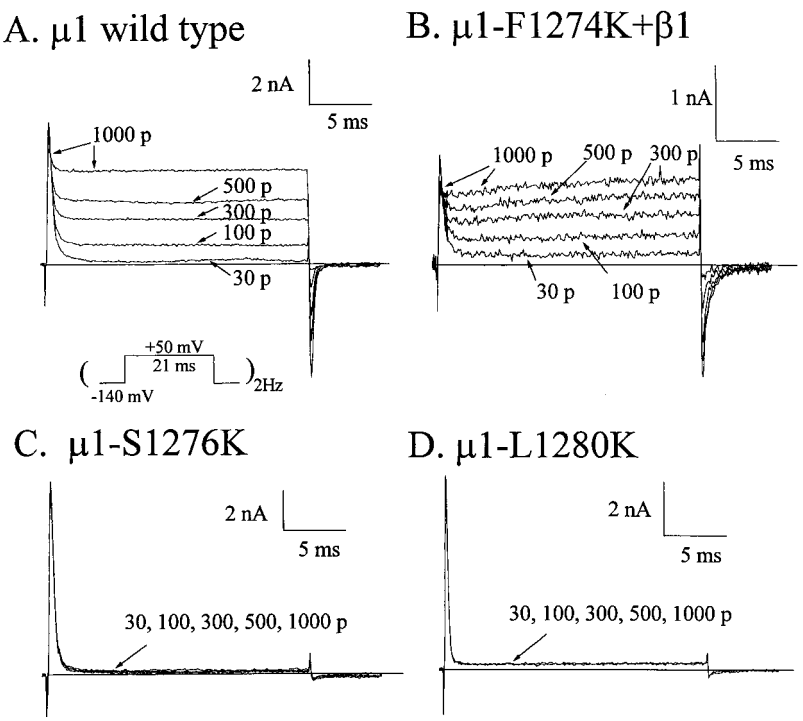

FIGURE 3 Outward Na^+ currents were recorded in HEK293t cells expressing either μ1 wild-type (*A*), μ1-F1274K (*B*), μ1-S1276K (*C*), or μ1-L1280K (*D*) channels with 5-μM BTX in the pipette under the ionic conditions described in Materials and Methods. Cotransfection of β1 subunit with μ1-F1274K was necessary to increase the level of expression. Cells were dialyzed by internal solution for 10–15 min with infrequent test pulses at +50 mV to determine the peak current amplitude until it reached steady state. Repetitive pulses (see *inset*) were then applied at 2 Hz, and the currents were recorded and superimposed for comparison. The pulse numbers are labeled; 30 p represents the 30 pulses applied to monitor Na^+ currents during cell dialysis. A small, varying amount of the noninactivating current at +50 mV present in some HEK293t cells (e.g., Fig. 1 *D*) was found in untransfected cells and was unrelated to voltage-gated Na^+ channels (Wang and Wang, 1998). A thin line drawn across the current traces depicts the current baseline.

activation kinetics. We found that both mutant channels remain functional but with substantial changes in their gating properties. Fig. 4*A* shows the conductance-voltage relationship of μ1, μ1-S1276K, and μ1-L1280K, whereas Fig. 4*B* shows the steady-state inactivation (h_∞ curve) of these channels. Activation was significantly shifted rightward in μ1-L1280K by ~22 mV ($p < 0.05$) and leftward in μ1-S1276K by ~12 mV ($p < 0.05$). Steady-state inactivation was not changed in μ1-S1276K and was shifted leftward in μ1-L1280K by ~12 mV ($p < 0.05$). We did not detect a measurable noninactivating component in the h_∞ curve (Fig. 4 *B*, >-60 mV). Furthermore, the lack of steady-state current in current traces (Fig. 5 *A*) suggests that fast inactivation reaches its completion during depolarization.

Reduced bupivacaine affinity for the inactivated state of BTX-resistant mutant channels

To test whether bupivacaine blocks BTX-resistant channels with a reduced affinity, we applied bupivacaine enantiomers to μ1 wild-type, μ1-S1276K, and μ1-L1280K mutant channels. We chose bupivacaine because it is widely used in the clinical setting. Bupivacaine blocks μ1 Na^+ channels in a voltage-dependent manner, as shown in Fig. 5 *A*. Details of bupivacaine block of wild-type μ1 Na^+ channels have been described (Nau et al., 1999) for somewhat different ionic conditions. A conditioning pulse with a duration of 10 s was applied to allow the drug to interact with the channel and to reach steady-state binding (Fig. 5, *top*). This conditioning pulse was followed by an interpulse duration of 100 ms at −140 mV to allow the drug-free channels to recover from their fast inactivation, and then a test pulse was applied to measure the availability of drug-free channels. The 100-ms interpulse does not allow drug-bound μ1 Na^+ channels to dissociate, because the time constant for recovery from the inactivated bupivacaine block is measured at 2.3 and 4.4 s, for 100 μM S(−)- and R(+)-bupivacaine, respectively (Nau et al., 1999). From −180 to −140 mV, the block reaches a constant value of ~55% at 100 μM R(+)-bupivacaine after normalization with the control peak current amplitude (Fig. 5, *top*). There is no stereoselectivity for the resting state, because the block is nearly the same with 100 μM S(−)-bupivacaine. From −80 to −50 mV, the block reaches a constant value of >90% at 100 μM R(+)-bupivacaine, probably through binding with the inactivated state (Nau et al., 1999). Again, the stereoselectivity remains minimal for μ1 wild-type channels. We estimated the resting affinity at −180 mV and the inactivated affinity at −50 mV for bupivacaine enantiomers, using the Langmuir isotherm, because the Hill coefficient was measured to be close to unity (Nau et al., 1999); the results of these estimates are listed in Table 1.

Under identical conditions, the mutant channels of μ1-S1276K and μ1-L1280K show significant differences in their voltage-dependent block. We noticed that μ1-S1276K mutant channels exhibit a conspicuous decrease in the control peak current by the 10-s conditioning pulses from −100 mV to −50 mV (Fig. 5 *B*, *middle*, *empty circles*), perhaps because of an enhanced slow inactivation. It is noteworthy

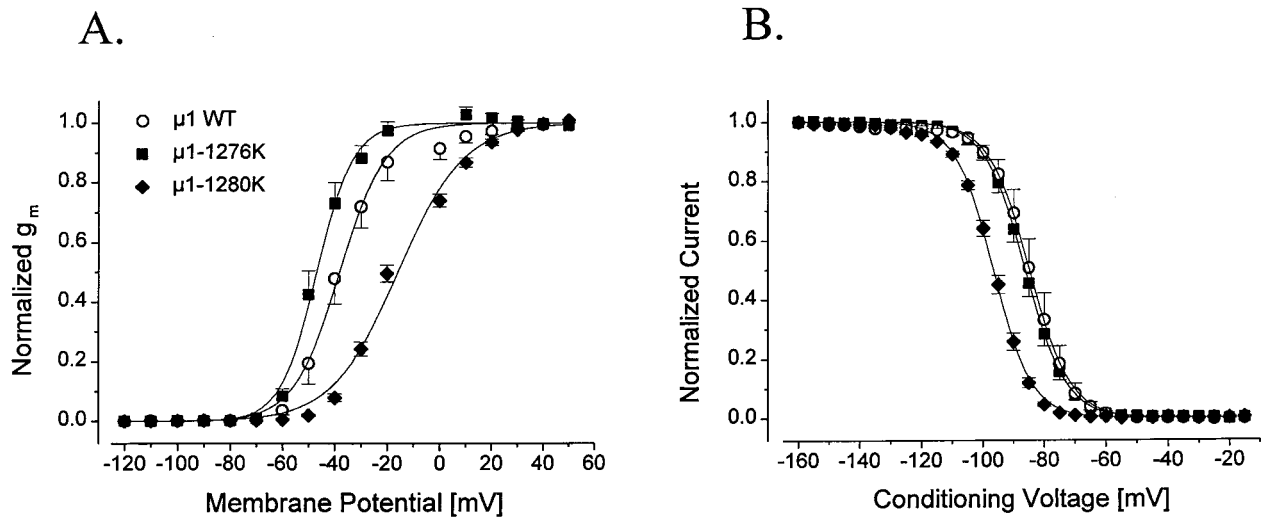

FIGURE 4 Voltage dependence of activation (*A*) and steady-state inactivation (*B*) was characterized in μ1 wild type (○), μ1-S1276K (■), and μ1-L1280K (◆). Cells were dialyzed by internal solution for ~20 min. The Na^+ current families were first measured at various voltages, and the peak conductance was estimated, $g = I_{Na}/(E - E_{rev})$, where I_{Na} is the peak current and E_{rev} is the estimated reversal potential, normalized and plotted against the corresponding voltage E and least-squares fitted (*solid lines*) with a Boltzmann equation, $g/g_{max} = 1\{1 + \exp(E_{0.5} - E)/k_a\}$, where $E_{0.5}$ is the voltage at which $g/g_{max} = 0.5$, k_a is the slope factor, and g_{max} is the maximum conductance. The fitted $E_{0.5}$ and k_a values, along with SEM of the individual fit, are -37.6 ± 3.3 mV and 8.5 ± 1.2 mV for wild type, -49.1 ± 3.1 mV and 5.9 ± 0.7 mV for μ1-S1276K, and -15.9 ± 1.5 mV and 12.4 ± 0.3 mV for μ1-L1280K, respectively ($n = 5$ or 6). The h_∞ curves were determined by a two-pulse protocol; Na^+ currents were evoked by a 5-ms test pulse to +30 mV after 100-ms conditioning pulses between −160 and −15 mV in 5-mV increments. Pulses were delivered at 20-s intervals. Peak currents were measured at the test pulse, normalized, and plotted against the prepulse conditioning potentials. The data were least-squares-fitted with a Boltzmann equation (*solid lines*), $y = 1/\{1 + \exp[(E_{pp} - h_{0.5})/k_h]\}$, where $h_{0.5}$ is the voltage at which $y = 0.5$ and k_h is the slope factor. The fitted $h_{0.5}$ and k_h values, along with SEM of the individual fit, are -84.8 ± 2.4 mV and 5.9 ± 0.1 mV for wild type, -86.3 ± 1.3 mV and 6.5 ± 0.3 mV for μ1-S1276K, and -96.7 ± 0.7 mV and 6.2 ± 0.1 mV, respectively ($n = 5$ or 6).

that the binding of bupivacaine reaches a constant level between −80 and −50 mV (Fig. 5 *B, middle, filled circles and squares*), where a progressive decrease in current by the 10-s conditioning pulse occurs. This current reduction phenomenon is similar to that found in mutants at the μ1-N434 position after various amino acid substitutions (Nau et al., 1999), but it likewise does not correlate with the bupivacaine potency. For μ1-S1276K, there are still two distinguishable binding affinities detected with this pulse protocol. The resting affinity of μ1-S1276K is reduced by 1.6- and 2.5-fold for R(+)- and S(−)-bupivacaine, respectively, compared with the wild type (Fig. 5, *middle*, and Table 1). The bupivacaine stereoselectivity ratio of resting block is increased in this mutant (1.4 versus 1.0 for wild type). In contrast, the inactivated affinities are reduced profoundly in μ1-S1276K mutant channels, and their bupivacaine stereoselectivity is reduced from a ratio of 1.5 to 1.0. The estimated K_I values show an ~10-fold reduction in the inactivated affinity of μ1-S1276K compared with that of the wild type (Table 1).

The difference in voltage-dependent block is even more drastic for μ1-L1280K than for μ1-S1276K. There appears to be no clear evidence of a voltage-dependent block by bupivacaine enantiomers from −180 to −50 mV (Fig. 5, *bottom*). The K_I affinity is no longer prevalent, thus demonstrating a reduction in inactivated affinity of ~15-fold. On the other hand, the resting affinity appears to be comparable to that of μ1-S1276K, with a reduction of approximately twofold compared with the estimates from the wild type (Table 1). Experiments using various concentrations of bupivacaine along with other amino acid substitution (Nau et al., 1999) will provide more accurate measurements of bupivacaine affinity as well as the chemical nature of bupivacaine binding with these two residues. Our results clearly indicate strong interactions between bupivacaine and the residues at μ1-S1276 and μ1-L1280 positions, particularly when the channel is in its inactivated state.

A state-dependent S6 model for BTX and LA binding reactions

It has been well demonstrated that overlapping receptors for drugs such as the alkylamines, the benz(othi)azepines, and the dihydropyridines are situated within segments D3-S6 and D4-S6 of L-type Ca^{2+} channels (for a review see Hockerman et al., 1997). These authors proposed a domain-interface binding model that readily explains the allosteric modulation of Ca^{2+} channels by these drugs. In contrast, we began with an assumption in our study that the receptors for BTX and LAs may be overlapped, and both may be situated on more than two homologous S6 segments within the

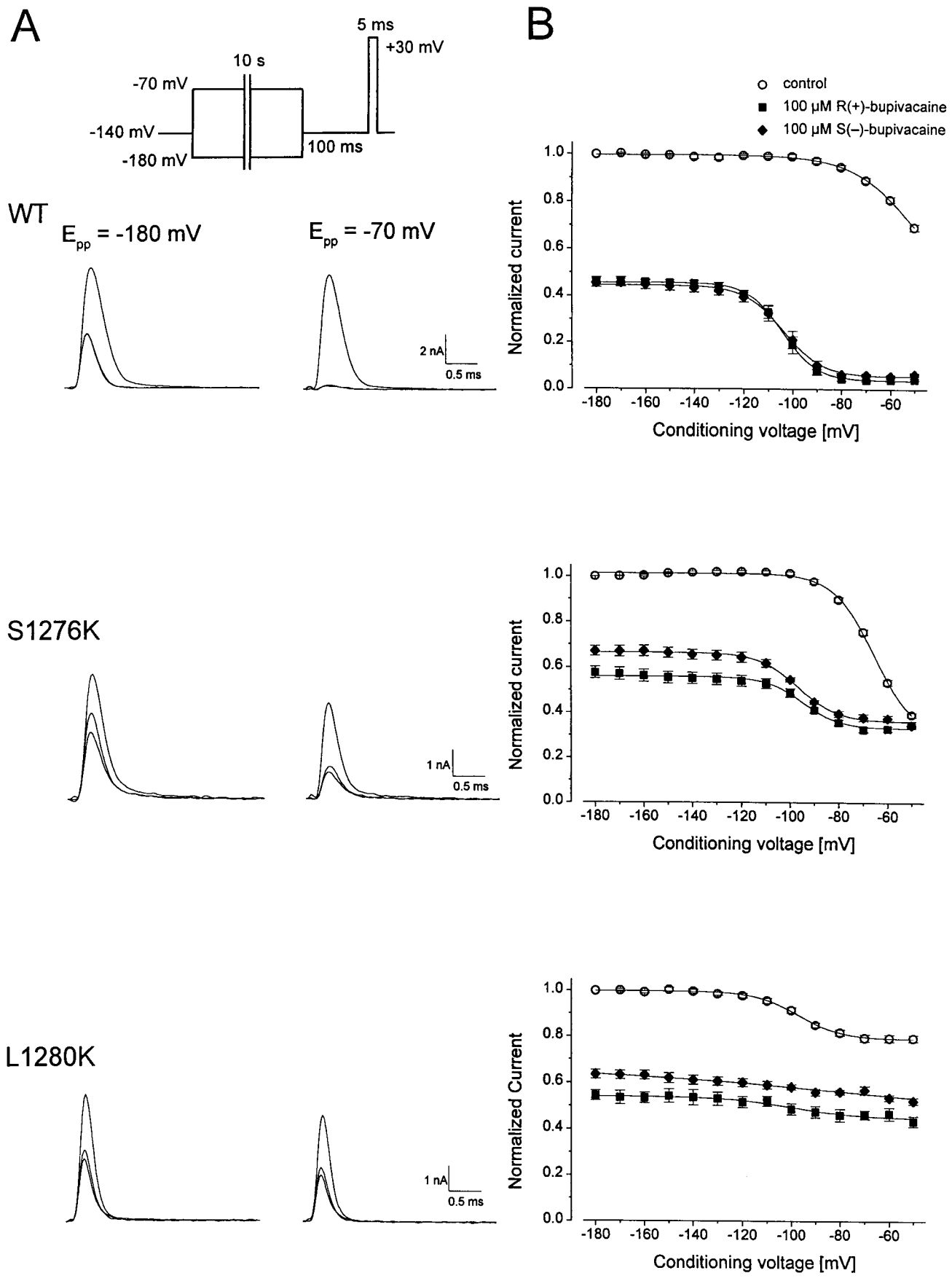
A
5 ms
+30 mV
10 s
-70 mV
-140 mV
-180 mV
100 ms
WT
E_pp = -180 mV
E_pp = -70 mV
2 nA
0.5 ms
B
control
100 µM R(+)-bupivacaine
100 µM S(–)-bupivacaine
Normalized current
Conditioning voltage [mV]
S1276K
1 nA
0.5 ms
Normalized current
Conditioning voltage [mV]
L1280K
1 nA
0.5 ms
Normalized Current
Conditioning voltage [mV]

TABLE 1 Relative binding affinities of bupivacaine enantiomers in μ1 wild-type, μ1-S1276K, and μ1-L1280K mutant channels

Channel types	Resting bupivacaine affinity K_R (μM)		S(−)/R(+) K_R ratio	Inactivated bupivacaine affinity K_I (μM)		S(−)/R(+) K_I ratio	K_R/K_I	
	R(+)	S(−)		R(+)	S(−)		R(+)	S(−)
μ1 wild type	84	83	1.0	4.6	7.0	1.5	18.3	11.9
μ1-S1276K (D3–S6)	136	204	1.4	54	53	1.0	2.5	3.8
μ1-L1280K (D3–S6)	120	174	1.5	78	110	1.4	1.5	1.6

The resting affinity (K_R) was estimated by an equation, relative $I_{Na} = K_R/[K_R + L]$, where L is 100 μM and relative I_{Na} is the normalized peak Na^+ current remaining at −180 mV after superfusion of bupivacaine. The inactivated affinity (K_I) was estimated by an equation, relative $I_{Na} = K_I/[K_I + L]$, where L is 100 μM and relative I_{Na} is the normalized peak Na^+ current remaining at −50 mV after drug superfusion. Relative I_{Na} values (mean of five experiments) were obtained from the results shown in Fig. 5.

intracellular vestibule. A negative outcome will support the notion that the receptors for BTX and for LAs are likely within the domain interface of D1-S6 and D4-S6 (Linford et al., 1998; Wang and Wang, 1999) with minimal interactions with other S6 segments. A positive result, however, will have additional structural implications. Such a result implies that all four homologous S6 segments align in close proximity at the BTX and LA receptor sites. One possibility for this close structural alignment is that these S6 segments may cross in α-helical bundles as an inverted teepee architecture, leaving an aperture at the bundle crossing, as shown in a bacterial K^+ channel (Doyle et al., 1998; Perozo et al., 1999). A similar tilted-S6 model including the bundle-crossing region as a putative activation gate has been proposed for the voltage-gated K^+ channel (Holmgren et al., 1998; del Camino et al., 2000). Using this analogous structural arrangement along with BTX and bupivacaine enantiomers as molecular probes, we account for our experimental results as follows.

First, BTX binds to its receptor only when the voltage-gated Na^+ channel is first in its open state. This finding is consistent with the state-dependent S6 binding model that the BTX receptor site is located on multiple S6 segments in close proximity, which may be somewhat constricted and/or are oriented unfavorably for BTX binding in the resting state. During channel activation, the BTX molecule binds to the channel in its open conformation and "stabilizes" such a state. Upon repolarization, BTX will remain bound and perhaps even "trapped" within the domain interface (D1/D4 and/or D3/D4) as the S6 segments return to their constricted resting state. The BTX binding energy released from its interaction with the open state of the Na^+ channel likely contributes to the hyperpolarizing shift of activation by 30–50 mV. This state-dependent S6 binding model adequately explains how BTX, upon binding to its receptor, can alter the activation gating of the Na^+ channel. Because the residues critical for BTX binding are located near the middle of S6 segments (Fig. 2), it is conceivable that the BTX receptor may be situated not far from the bundle-crossing region, which may in turn function like an activation gate. Perhaps because of its constricted receptor site, BTX also does not bind significantly when the Na^+ channel is in the inactivated state (Tanguy and Yeh, 1991).

Second, in the resting state LAs interact weakly with their receptor, presumably at the D4-S6 segment alone (Ragsdale et al., 1994), probably because the two adjacent S6 segments are not in a close position for binding with LAs. In the inactivated state these S6 segments may move and/or rotate inward. The small bupivacaine molecule is now able to interact with additional residues from all three S6 segments, thus establishing a binding affinity that is more than 10-fold greater (Table 1). As a result, the LA molecule "stabilizes" these three S6 segments in their inactivated state. The binding energy released from these additional contacts provides the stabilization. This chemical stabilization concept is in accord with Hille's modulated receptor hypothesis (Hille, 1977). When a lysine residue is introduced at the LA receptor site, such chemical stabilization is reduced significantly because of the presence of a positive charge (Fig. 5 and Table 1). According to this S6 binding model, μ1-S1276 and μ1-L1280 (at D3-S6), along with μ1-N434, μ1-L437 (at D1-S6), μ1-F1579, and μ1-Y1586 (at D4-S6), line the permeation pathway when the channel is in its inactivated state. How these individual S6 segments are modulated by the Na^+ channel fast inactivation is unclear. Nonetheless, our state-dependent S6 binding model suggests that the inactivation gating is linked to the LA receptor somewhere along the α-helical structure of at least

FIGURE 5 Steady-state block of μ1 wild-type (*top*), μ1-S1276K (*middle*), and μ1-L1280K (*bottom*) Na^+ channels by bupivacaine enantiomers. (*A*) Representative superimposed Na^+ current traces were recorded before and after each application of bupivacaine enantiomers at a conditioning voltage E_{pp} of either −180 mV (*left traces*) or −70 mV (*right traces*) for 10 s. The pulse protocol is detailed at the top. (*B*) Peak Na^+ currents were measured before (*large outward current traces in A*) and after (*smaller outward current traces in A*) each drug application, normalized with respect to the peak current amplitude at −180 mV, and plotted against E_{pp}. The drug-treated data were renormalized with the control value without the drug (○) to yield the relative block of peak Na^+ currents ($n = 5$).

one of four S6 segments. In fact, only 22 residues separate the IFM locus of the putative inactivation particle (at position μ1-I1303-M1305 within D3-D4 linker) from the μ1-L1280 position (D3-S6). It appears that the LA receptor itself may not be in direct contact with the inactivation machinery, because the position of the fast-inactivation gate is not affected by the LA lidocaine during recovery from the inactivated state (Vedantham and Cannon, 1999).

CONCLUSION

Our state-dependent S6 binding model with multiple S6 segments participating intimately in BTX and LA binding interactions provides adequate explanations for the experimental results described here. Although imprecise in molecular terms, this working model clearly implies that the S6 segments can readily change their relative positions during state transitions. Particularly appealing is the possibility that S6 segments may include a bundle-crossing region. It will be interesting to determine whether such a region exists as an activation gate in the Na^+ channel. Evidently, the BTX receptor within S6 segments must somehow be able to modify the activation, fast inactivation, and slow inactivation gating, inasmuch as the binding of BTX profoundly alters these gating processes. Likewise, the LA receptor, when bound to LAs, appears to stabilize the inactivated state of Na^+ channels (Hille, 1977), although such stabilization may be through an indirect mechanism. The receptor sites for BTX and LAs are in these dynamic S6 regions, and consequently their binding interactions with these ligands are highly state dependent.

We are grateful to Drs. John Daly and Rune Sandberg for providing BTX and bupivacaine enantiomers, respectively.

This work was supported by National Institutes of Health grants GM-35401 and GM-48090.

REFERENCES

Balser, J. R., H. B. Nuss, N. Chiamvimonvat, M. T. Perez-Garcia, E. Marban, and G. F. Tomaselli. 1996. External pore residue mediates slow inactivation in μ1 rat skeletal muscle sodium channels. *J. Physiol. (Lond.).* 494:431–442.

Bean, B. P. 1992. Whole-cell recording of calcium channel currents. *Methods Enzymol.* 207:181–193.

Bennett, E. S. 1999. Effects of channel cytoplasmic regions on the activation mechanisms of cardiac versus skeletal muscle Na^+ channels. *Biophys. J.* 77:2999–3009.

Brown, G. B. 1988. Batrachotoxin: a window on the allosteric nature of the voltage-sensitive sodium channel. *Int. Rev. Neurobiol.* 29:77–116.

Burke, D., D. J. Henderson, A. M. Simpson, K. A. Faccenda, L. M. Morrison, E. M. McGrady, G. A. McLeod, and J. Bannister. 1999. Comparison of 0.25% S(−)-bupivacaine with 0.25% RS-bupivacaine for epidural analgesia in labour. *Br. J. Anaesth.* 83:750–755.

Cannon, S. C. and S. M. Strittmatter. 1993. Functional expression of sodium channel mutations identified in families with periodic paralysis. *Neuron.* 10:317–326.

Catterall, W. A. 1980. Neurotoxins that act on voltage-sensitive sodium channels in excitable membranes. *Annu. Rev. Pharmacol. Toxicol.* 20: 15–43.

Catterall, W. A. 1995. Structure and function of voltage-gated ion channels. *Annu. Rev. Biochem.* 64:493–531.

Chandler, W. K., and H. Meves. 1970. Slow changes in membrane permeability and long-lasting action potentials in axons perfused with sodium fluoride. *J. Physiol. (Lond.).* 211:707–728.

Creveling, C. R., E. T. McNeal, J. W. Daly, and G. B. Brown. 1983. Batrachotoxin-induced depolarization and [^{3}H]batrachotoxinin-A 20α-benzoate binding in a vesicular preparation from guinea pig cerebral cortex: inhibition by local anesthetics. *Mol. Pharmacol.* 25:350–358.

Daly, J. W., C. W. Myers, and J. E. Warnick. 1980. Levels of batrachotoxin and lack of sensitivity to its action in poison-dart frogs (*Phyllobates*). *Science.* 208:1383–1385.

del Camino, D., M. Holmgren, Y. Liu, and G. Yellen. 2000. Blocker protection in the pore of a voltage-gated K^+ channel and its structural implications. *Nature.* 403:321–324.

Doyle, D. A., J. M. Cabral, R. A. Pfuetzner, A. Kuo, J. Gulbis, S. Cohen, B. T. Chait, and R. MacKinnon. 1998. The structure of the potassium channel: molecular basis of potassium conduction and selectivity. *Science.* 280:69–77.

Fozzard, H. A., and D. A. Hanck. 1996. Structure and function of voltage-dependent sodium channels: comparison of brain II and cardiac isoforms. *Physiol. Rev.* 76:887–926.

Hamill, O. P., E. Marty, M. E. Neher, B. Sakmann, and F. J. Sigworth. 1981. Improved patch-clamp techniques for high-resolution current recording from cells and cell-free membrane patches. *Pflugers Arch.* 391:85–100.

Hanck, D. A., J. C. Makielski, and M. F. Sheets. 1994. Kinetic effects of quaternary lidocaine block of cardiac sodium channels: a gating current study. *J. Gen. Physiol.* 103:19–43.

Hille, B. 1977. Local anesthetics: hydrophilic and hydrophobic pathways for the drug receptor reaction. *J. Gen. Physiol.* 69:497–515.

Hille, B. 1992. Ionic Channels of Excitable Membranes. Sinauer Associates, Sunderland, MA.

Hockerman, G. H., B. Z. Peterson, B. D. Johnson, and W. A. Catterall. 1997. Molecular determinants of drug binding and action on L-type calcium channels. *Annu. Rev. Pharmacol. Toxicol.* 37:361–396.

Holmgren, M., K. S. Shin, and G. Yellen. 1998. The activation gate of a voltage-gated K^+ channel can be trapped in the open state by an intersubunit metal bridge. *Neuron.* 21:617–621.

Linford, N. J., A. R. Cantrell, Y. Qu, T. Scheuer, and W. A. Catterall. 1998. Interaction of batrachotoxin with the local anesthetic receptor site in transmembrane segment IVS6 of the voltage-gated sodium channel. *Proc. Natl. Acad. Sci. USA.* 95:13947–13952.

McPhee, J. C., D. S. Ragsdale, T. Scheuer, and W. A. Catterall. 1998. A critical role for the S4–S5 intracellular loop in domain IV of the sodium channel α-subunit in fast inactivation. *J. Biol. Chem.* 273:1121–1129.

Nau, C., S.-Y. Wang, G. R. Strichartz, and G. K. Wang. 1999. Point mutations at N434 in D1–S6 of μ1 Na^+ channels modulate potency and stereoselectivity of local anesthetic enantiomers. *Mol. Pharmacol.* 56: 404–413.

Perozo, E., D. M. Cortes, and L. G. Cuello. 1999. Structural rearrangements underlying K^+-channel activation gating. *Science.* 285:73–78.

Postma, S. W., and W. A. Catterall. 1984. Inhibition of binding of ^{3}H batrachotoxin A 20-α-benzoate to Na channels by local anesthetics. *Mol. Pharmacol.* 25:219–227.

Ragsdale, D. S., J. C. McPhee, T. Scheuer, and W. A. Catterall. 1994. Molecular determinants of state-dependent block of Na^+ channels by local anesthetics. *Science.* 265:1724–1728.

Smith, M. R. and A. L. Goldin. 1997. Interaction between the sodium channel inactivation linker and domain III S4–S5. *Biophys. J.* 73: 1885–1895.

Strichartz, G. R., T. A. Rando, and G. K. Wang. 1987. An integrated view of the molecular toxicology of sodium channel gating in excitable cells. *Annu. Rev. Neurosci.* 10:237–267.

Sunami, A., S. C. Dudley, and H. A. Fozzard. 1997. Sodium channel selectivity filter regulates antiarrhythmic drug binding. *Proc. Natl. Acad. Sci. USA.* 94:14126–14131.

Tanguy, J. and J. Z. Yeh. 1991. BTX modification of Na channels in squid axons. I. State dependence of BTX action. *J. Gen. Physiol.* 97:499–519.

Trainer, V. L., G. B. Brown, and W. A. Catterall. 1996. Site of covalent labeling by a photoreactive batrachotoxin derivative near transmembrane segment IS6 of the sodium channel α subunit. *J. Biol. Chem.* 271:11261–11267.

Ukomadu, C., J. Zhou, F. J. Sigworth, and W. S. Agnew. 1992. μl Na^+ channels expressed transiently in human embryonic kidney cells: biochemical and biophysical properties. *Neuron.* 8:663–676.

Vedantham, V., and S. C. Cannon. 1999. The position of the fast-inactivation gate during lidocaine block of voltage-gated Na^+ channels. *J. Gen. Physiol.* 113:7–16.

Vilin, Y. Y., N. Makita, A. L. George, and P. C. Ruben. 1999. Structural determinants of slow inactivation in human cardiac and skeletal muscle sodium channels. *Biophys. J.* 77:1384–1393.

Wang, G. K., M. S. Brodwick, D. C. Eaton, and G. R. Strichartz. 1987. Inhibition of sodium currents by local anesthetics in chloramint-T treated squid axons. *J. Gen. Physiol.* 89:645–667.

Wang, G. K., C. Quan, and S.-Y. Wang. 1998. Local anesthetic block of batrachotoxin-resistant muscle Na^+ channels. *Mol. Pharmacol.* 54: 389–396.

Wang, S.-Y., and G. K. Wang. 1998. Point mutations in segment I-S6 render voltage-gated Na^+ channels resistant to batrachotoxin. *Proc. Natl. Acad. Sci. USA.* 95:2653–2658.

Wang, S.-Y., and G. K. Wang. 1999. Batrachotoxin-resistant Na^+ channels derived from point mutations in transmembrane segment D4–S6. *Biophys. J.* 76:3141–3149.

West, J. W., D. E. Patton, T. Scheuer, Y. Wang, A. L. Goldin, and W. A. Catterall. 1992. A cluster of hydrophobic amino acid residues required for fast Na^+ channel inactivation. *Proc. Natl. Acad. Sci. USA.* 89: 10910–10914.

Yang, N., A. L. George, and R. Horn. 1996. Molecular basis of charge movement in voltage-gated sodium channels. *Neuron.* 16:113–122.